FRACTURE CHARACTERISTICS AND SIZE EFFECT IN NORMAL AND HIGH-STRENGTH CONCRETE BEAM

S.H. Eo
Dept. of Civil Engrg., Changwon National Univ., Changwon, Korea
N.M. Hawkins and G.S. Kwak
Dept. of Civil Engrg., Univ. of Illinois at Urbana-Champaign, Illinois, USA

Abstract

A finite element numerical analysis, using a bilinear fictitious crack model (FCM), was made to investigate size effect predictions for normal-strength concrete (NSC) and high-strength concrete (HSC) three-point bend specimens with and without an initial crack. Based on the numerical results a simple size effect equation was proposed and compared with the predictions of equations proposed by others. It is concluded that fracture characteristics and notch characteristics need to be included in size effect relationships.

1 Introduction

The major difference between the fracture behavior of high- and normal-strength concrete (NSC) is caused by differences in the degree of aggregate interlock that accompanies cracking. For instance, HSC has a high tensile strength, but cracking passes through, rather than around the aggregate, producing less fracture energy for unit crack extension (G_F) than NSC. This means that the behavior of HSC can not be characterized by the strength properties of the concrete alone. Additional material properties such as the fracture energy and the strain-softening diagram are needed for

precise predictions of the fracture behavior of important structures constructed with HSC.

Numerous experimental investigations have shown that the presence of the so-called fracture process zone (FPZ), located between the front of the traction-free crack and the tip of the visible crack, is the major determinant of the nonlinear fracture behavior of concrete, and that the fracture process itself is dependent upon the relative size and the shape of the specimen. Small sized specimens tend to fail by plastic collapse, while the large sized specimens fail by brittle fracture. Such a transition in failure modes with change in structural size has also been demonstrated by Petersson (1981), Bazant and Cedolin (1979) and Carpinteri (1990) through extensive numerical simulations of crack propagation in a three-point bend test specimens.

The purpose of this paper is to quantitatively investigate size effects for HSC beams with and without initial cracks (or notches). For this purpose, fracture characteristics such as the softening behavior and the presence of a large-sized process zone ahead of the traction-free crack are analyzed using finite element method and the fictitious crack approach developed by Hillerborg et al. (1976). Based on the numerical results, size effect formula are proposed and compared for NSC and HSC specimens.

2 Numerical investigation based on FCM

The numerical scheme in this study relies on the use of the superposition principle suggested by Gopalaratnam and Ye (1991) to obtain solutions to the inelastic problem, without the need to iterate, by effectively treating the nonlinearities caused by the process zone as a traction boundary.

To investigate fracture characteristics and size effects for HSC, geometrically similar specimens of five different sizes were analyzed assuming three different levels of concrete strength. The depths of the beams were taken as 100, 200, 400, 800 and 1600 mm and the width was held constant at 100 mm. Span to depth ratios were taken as 4. The notch-length to beam-depth ratio, a_0/d, was varied from 0 to 0.5 by increments of 0.1. The material properties, i.e., Young's modulus (E) and softening diagram were chosen as average value obtained through a parametric study. For that study, the complete load-deflection curves measured by Nomura et al. (1990) were simulated using the results of finite element analyses and a FCM.

Four parameters, f_t, σ_1, w_1 and w_c are necessary to describe the bilinear softening diagram. The material properties and the parameters obtained from the analysis of Nomura et al.'s results are given in Table 1. The letters NSC, MSC and HSC are used to differentiate between the three different concrete strengths. Shown in Fig.1 is the specimen configuration and the finite element mesh used for the numerical investigation. Since the loading was symmetrical, it was necessary to model half the beam only.

Table 1. Material properties and model parameters obtained from analyses of Nomura et al.'s test results.

	f_t (MPa)	σ_1 (MPa)	w_1 (mm)	w_c (mm)	E (MPa)	G_F (N/m)	l_{ch} (mm)
NSC	2.51	0.50	0 .0175	0.174	32000	65.5	332.7
MSC	3.77	1.10	0.0125	0.085	45000	70.3	222.6
HSC	5.14	1.20	0.0100	0.047	60000	53.9	122.4

The results of Table 1 show clearly some of the difficulties that can be anticipated with the use of high strength concretes. As the tensile strength increases, critical crack opening values decrease, and therefore the fracture energy does not increase.
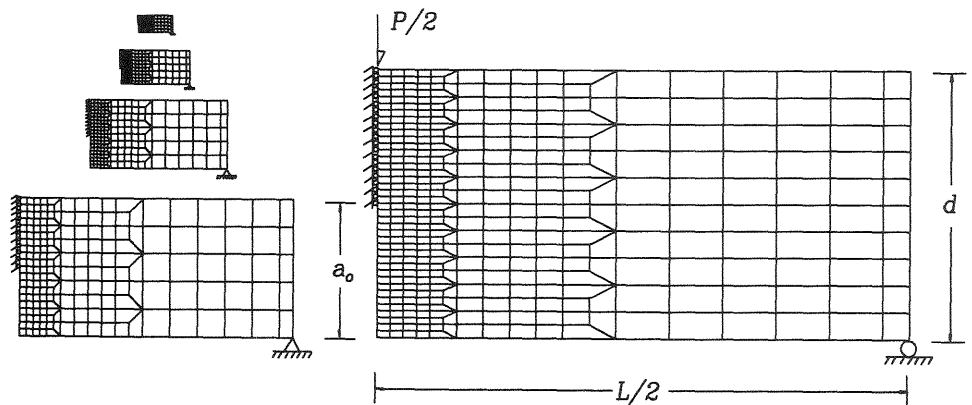
Specimen size : d=100, 200 mm
No. of element = 195
No. of d.o.f. = 450
No. of node on crack line = 20

Specimen size : d=400, 800, 1600 mm
No. of element = 390
No. of d.o.f. = 864
No. of node on crack line = 40

Fig. 1. Specimen configuration and finite element mesh used for the numerical investigation.

3 Analysis of the results

3.1 Load carrying capacity and softening behavior

The material properties of Table 1 were used in conjunction with the mesh of Fig. 1 to calculate load-deflection curves for beams of varying geometry and varying notch depth. Typical resultant curves are shown in Fig. 2. For deep initial notches, stiffness and loading capacity decrease, whereas ductility increases. The slope of the softening branch is a maximum when the beam is initially uncracked. The general trend for varying notch depth ratios is the same for beams of different depths. However, for beam depths greater than 400 mm in case of NSC and 200 mm in case of HSC, instability in the fracture process can be expected as the softening slope presents increasingly positive initial values with increasing beam size and decreasing a_0/d ratio. This size-scale transition from ductile to catastrophic failure has been analyzed extensively by Carpinteri (1990). He pointed out that a critical size-scale exists for which the softening slope is infinite and a bifurcation point can be demonstrated by use of the simple LEFM condition that K_1 equals K_{1c}.
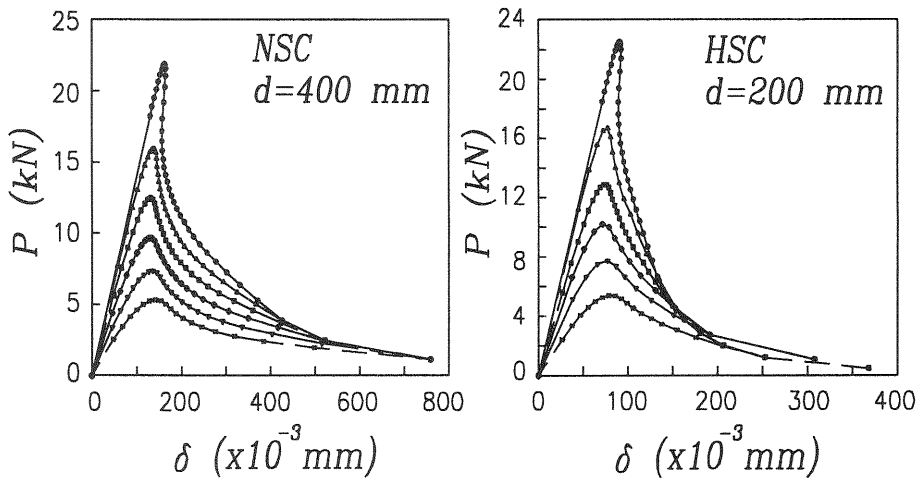

Fig. 2. Typical load-deflection curves obtained for NSC and HSC beams.

Shown in Fig. 3 is a comparison of the load carrying capacity predicted by the FCM and by LEFM as a function of the brittleness number d/l_{ch}, where $l_{ch}=EG_F/f_t^2$. In Fig. 3, P_u^{FCM} values were obtained from P-δ curves and the maximum load P_u^{LEFM} according to LEFM was derived from the formula by Tada et al. (1973).
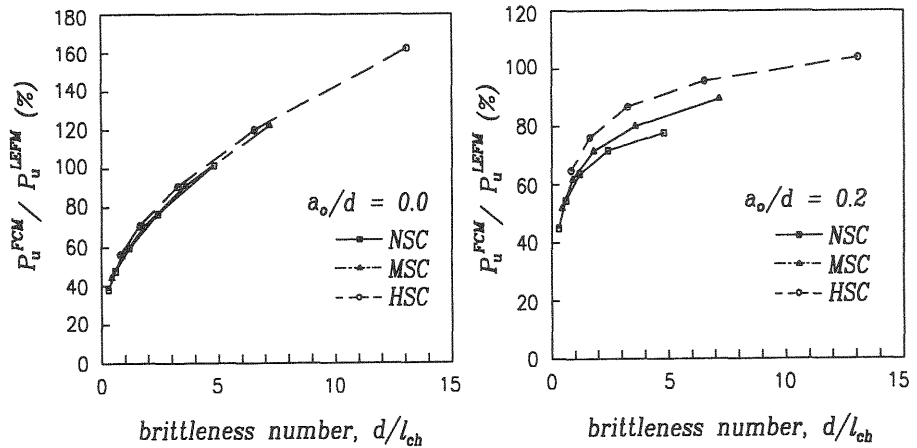
Fig. 3. Comparison of load-carrying capacities according to FCM and LEFM for NSC, MSC and HSC: (a) $a_0/d = 0$; (b) $a_0/d = 0.2$

As apparent from Fig. 3, the results of the FCM tend to those of LEFM for low l_{ch}, i.e., the lower the fracture energy, the larger the beam size d and/or the higher the tensile strength f_t, the more closely the results can be predicted by LEFM. Further, the asymptotic trend towards the LEFM prediction is more rapid in the case of HSC than NSC. Also, the value of P_u^{FCM}/P_u^{LEFM} is larger than unity for unnotched beams. This fact means that the load carrying capacity approaches gradually the prediction by LEFM for increasing brittleness, but has an asymptotic limit beyond a certain value of the brittleness number for unnotched beams including HSC beams. This result is important for the derivation of a size effect formula for uncracked concrete beams as discussed later.

3.2 Size effects for unnotched and notched specimens

A nominal strength, σ_N, for comparison purposes, can be obtained by dividing the maximum load by the cross-section area (total or ligament area) of the beam. Shown in Fig. 4 are the numerical results and the curves determined using Bazant's size effect law (broken lines) (1984) and the formula (unbroken line) suggested by one of the authors (1990) for concrete specimens without an initial notch. It is evident from Fig. 4 that the trend in size effects is greatly different for cracked and uncracked specimens. Consequently, the Bazant's size effect law, which is theoretically valid for geometrically similar specimens with the same relative crack length, a/d, must be modified to a form which can describe the size effect trend for uncracked specimens, namely,

$$\sigma_N = \frac{B \cdot f_t}{\sqrt{1 + d/d_o}} + \alpha \cdot f_t \tag{1}$$

where B, d_o and α are empirical constants which can be obtained from nonlinear regression analysis of the numerical results.
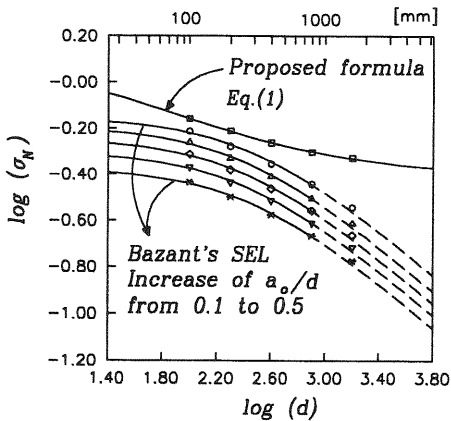

Fig. 4. Numerical results and curve fitting with Bazant's SEL for notched NSC beams and with Eq. (1) for unnotched beams.

3.3 Size effects for different strength of concrete

As discussed in the previous section, Eq. (1) provides a good estimate for size effects in concrete specimens without an initial crack. In this section, Eq. (1) is also applied for estimating size effects for the flexural strength of concrete when specimens have different levels of concrete strength. The flexural strength f_{net} is the value obtained by dividing the maximum bending moment by the section modulus. i.e., $f_{net} = M_{max}/Z = 6\sigma_N$.

Uchida et al. (1992) have proposed an empirical equation for size effects by investigating various equations and expressing them in a simple form, given by Eq. (2) :

$$\frac{f_{net}}{f_t} = 1 + \frac{1}{0.85 + 4.5(d/\ell_{ch})} \tag{2}$$

where $d/\ell_{ch} \geq 0.1$ is suggested as a result of that study. On the other hand, the relationship between flexural strength and uniaxial tensile strength specified in the CEB-FIP model code 1990, is given by Eq. (3) :

$$\frac{f_{net}}{f_t} = \frac{1 + 2.0(d/d_o)^{0.7}}{2.0(d/d_o)^{0.7}} \tag{3}$$

690

where $d \geq 50$ mm and $d_0 = 100$ mm.

Comparisons of the three estimations given by Eqs. (1), (2) and (3) with the numerical results are shown in Fig. 5. It can be concluded from Fig. 5 that the flexural strength decreases with increasing beam size and that HSC attains its limiting value more rapidly than lower strength concrete. For NSC in the range of $d \geq 50$ mm as specified in CEB-FIP Model Code, all of the three equations give good estimations. For HSC, the estimates from Eqs. (1) and (3) are almost the same in the range of $d \geq 50$ mm, while Eqs. (2) and (3) give the same result for NSC in the same range.
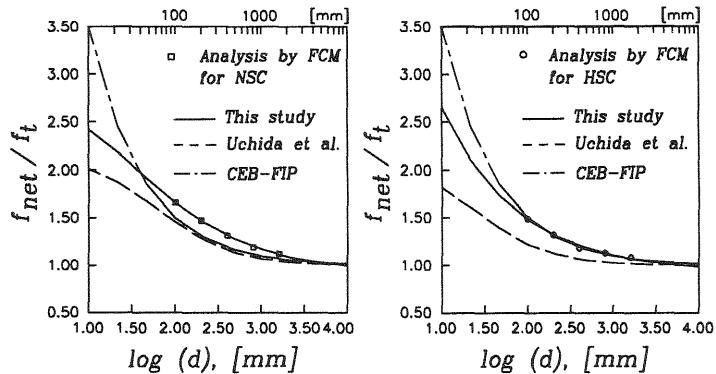

Fig. 5. Comparison of the equations for prediction of the flexural strength of concrete: (a) NSC; (b) HSC.

4 Conclusions

The finite element numerical investigations conducted in this study gave good results for the load carrying capacity and softening behavior of HSC as well as NSC. Suggested equation shows a good agreement with the numerical results for size effect predictions for unnotched beams, while Bazant's size effect law does not.

From the size effect analyses for flexural strength reported here, it appears that size effects attain their limiting values more rapidly for HSC than for NSC and MSC. Comparisons made using the three different equations showed all reasonable estimates for size effects for flexural strength for NSC, while deviations between the proposed equation and the other two equations increased for HSC.

Physical tests are needed to determine which size effect relationship is most applicable for HSC.